Electronic Supplementary Material (ESI) for Physical Chemistry Chemical Physics.

Electronic Supplementary Information

DNP-Enhanced Solid-State NMR Yields Precise Details on Atom Ordering in Amorphous Silica-Alumina

Frédéric A. Perras,[a] Zichun Wang,[b] Takeshi Kobayashi,[a] Alfons Baiker,[c] Jun Huang,*[b]

Marek Pruski*[a,d]

[a]US DOE, Ames Laboratory, Ames, IA 50011, USA

[b]Laboratory for Catalysis Engineering, School of Chemical and Biomolecular Engineering & Sydney Nano Institute, University of Sydney, Sydney, NSW 2006, Australia

[c]Institute for Chemical and Bioengineering, Department of Chemistry and Applied Bioscience, ETH Zürich, HCI, CH-8093, Switzerland

[d]Department of Chemistry, Iowa State Unviersity, Ames, IA 50011, USA

Sample preparation

The preparation of the ASAs was carried out at ca. 2000 K in a very quick FSP process (on the order of milliseconds) which combines the synthesis and calcination steps.[2] In short, the appropriate amounts of the Al precursor (aluminum acetylacetonate, 99%, ABCR) and Si precursor (tetraethoxysilane, 99%, Fluka) materials were dissolved in a 1:1 (vol.%) mixture of acetic acid (analytical grade, Fluka) and methanol (analytical grade, Fluka). The resulting solution was filtered using a glass filter, pumped through a capillary at a rate of 5 $mLmin^{-1}$, nebulized at 5 $Lmin^{-1}$ O_2, and ignited by an annular methane/oxygen flame (1.5/0.9 $Lmin^{-1}$) to generate ASA nanoparticles. Assisted by a Busch SV 1040C vacuum pump, particles were collected on a cooled Whatman GF6 filter (257 mm diameter).

An ^{17}O-enriched ASA/50 sample was also prepared by first dehydrating the unenriched sample at 723 K for 12 h, under vacuum, and then heating it in an $^{17}O_2$ gas (90 atom%, Aldrich) atmosphere at 853 K for 12 h on a vacuum line, as previously reported.[1] As previously demonstrated[1] we used ^{1}H-^{17}O TRAPDOR in order to estimate the surface ^{17}O enrichment of the material. The dephasing observed (see Figure S10) suggests a surface ^{17}O enrichment of ~30%. ^{27}Al SSNMR measurements were used to confirm that the integrity of the structure was maintained during this process (see Figure S9).

N_2 Physisorption

The surface areas of the ASA materials were determined by N_2 adsorption/desorption isotherms on an Autosorb IQ-C system. An amount of 50 mg of each sample was degassed at 423 K for 12 h under vacuum before the measurements and then recorded at 77 K using the BET method. The BET surface areas for all the materials are given in Table S1.

Table S1. Surface properties of ASA catalysts

	Surface area ($m^2.g^{-1}$)	BAS [a] ($mol.g^{-1}$)
ASA/70	200	15.1×10^{-2}
ASA/50	222	13.4×10^{-2}
ASA/30	248	11.1×10^{-2}
ASA/10	377	9.8×10^{-2}

[a]The number of BASs of ASA samples were obtained from ref [2] and are consistent with the values determined also in ref [3].

Electron microscopy

Elemental mapping of aluminum and silicon was done using energy-dispersive X-ray spectroscopy (EDX) measurements performed on the FEI Titan Themis Cubed aberration corrected STEM microscope housed at the Ames Laboratory's Sensitive Instrument Facility, operated at an accelerating voltage of 200 kV. Samples were prepared by placing 2 drops of ethanol suspensions

[1] L. Peng, Y. Liu, N. Kim, J. E. Readman and C. P. Grey, *Nat. Mater.* 2005, **4**, 216-219.

[2] J. Huang, N. van Vegten, Y. Jiang, M. Hunger and A. Baiker *Angew. Chem. Int. Ed.* 2010, **49**, 7776-7781.

[3] Z. Wang, Y. Jiang, O. Lafon, J. Trébosc, K. D. Kim, C. Stampfl, A. Baiker, J.-P. Amoureux and J. Huang *Nature Commun.* 2016, **7**, 13820.

of the powders onto lacey carbon-coated copper grids which were then allowed to dry at room temperature for several days.

The STEM and EDX images of the six materials discussed in the main text are shown below in Figures S4-S7. No large segregated alumina or silica phases could be detected in any of the samples, and thus the phases that were detected by NMR must be composed of very small domains that are invisible to EDX. Similarly, no crystalline particles were observed. In all samples the Si:Al ratio was within 10% of the synthesis values. However, we were able to observe regions with locally increased Si or Al concentration, which in most samples deviated from the average concentration by no more than 10%. This is in agreement with the slight segregation we noted from our NMR measurements. In one of the samples, ASA/10, we additionally noticed the formation of isolated silica-alumina nanoparticles (see Figure S4), which have Si:Al ratios of 50:50. No electron diffraction could be detected from these particles and they are thus non-crystalline. The origin of these particles is unknown but they are not expected to meaningfully contribute to the catalytic activity due to their far lower surface areas. These particles' effects on the ^{29}Si{^{27}Al} RESPDOR measurements couldn't be detected and thus it is reasonable to state that RESPDOR measurements are only sensitive to the average aluminum concentration.

Powder X-ray diffraction

Powder X-ray diffraction (XRD) patterns were acquired for all samples at room temperature using a Rigaku X-ray diffractometer equipped with a Mo kα X-ray source (λ = 0.7107 Å). The samples were scanned from 5 to 30° in steps of 0.02° at a rate of 4 s per step. No reflections could be detected in any of the samples, in agreement with the NMR and EDX data which indicate that these materials are amorphous (Figure S8).

1D and 2D ^{29}Si MAS NMR

^{29}Si{^{1}H} 1D cross-polarization (CP)MAS spectra were acquired at an MAS spinning frequency of 6 kHz, using a 2.5 μs ^{1}H excitation pulse and a 4 ms contact time. Between 8 and 32 scans were accumulated, using a recycle delay between 2.4 and 8 s, depending on the sample. The delay was set at 1.3T_1, as measured using a saturation recovery experiment. ^{29}Si 2D DQ/SQ spectra were acquired using the same parameters as the CPMAS spectra, and the POST-C7 recoupling sequence[4] was used to excite the DQ transitions. The t_1 increments were rotor-synchronized and between 14 and 24 t_1 increments, each consisting of between 128 and 1152 scans, were accumulated using the States-TPPI method for phase-sensitive detection.

Contrary to ^{27}Al spectra, the 1D ^{29}Si SSNMR spectra of aluminosilicates are sensitive to the second coordination sphere. In low surface area materials, ^{29}Si spectra can be deconvoluted into five overlapping resonances that are assigned to Q$^{(4)}$ sites connected to between 0 and 4 aluminum sites, with each Al substitution leading to a 5 ppm increase in the ^{29}Si chemical shift.[5] We did observe a shift of the ^{29}Si resonance towards higher chemical shift in our ASA samples (see Figure S4) as the aluminum content was increased, indicating the formation of a larger number of Si-O-

[4] M. Hohwy, H. J. Jakobsen, M. Edén, M. H. Levitt and N. C. Nielsen, *J. Chem. Phys.* 1998, **108**, 2686-2694.
[5] J. Ren, L. Zhang and H. Eckert *J. Phys. Chem. C* 2014, **118**, 4906-4917.

Al linkages. In particular, the elevated shift of the ^{29}Si resonance in ASA/70, suggests the formation of a significant number of Si(3Al) sites.[4] DNP-enhanced ^{29}Si DQ/SQ experiments[6-7] were applied to further investigate silicon clustering, as was done for aluminum. While the one-dimensional spectra are incapable of yielding information regarding the formation of local domains, these can be seen by ^{29}Si-^{29}Si correlation. A non-homogeneous mixture of silicon and aluminum would lead to the formation of ridges in the 2D spectra[8,9] while a homogeneous distribution would yield spectra with round features, where every ^{29}Si shift is correlated to every other ^{29}Si shift. For both classes of samples, the spectra were consistent with a homogeneous mixture of silicon sites (Figure S2). An enlarged view of Figure 3 from the main text is also given as Figure S3.

RESPDOR simulation model details

In the case of REDOR, the total recoupling curve is then given by:

$$\frac{\Delta S}{S_0} = 1 - \frac{1}{4\pi}\int_0^{2\pi}\int_0^{\pi}\int_0^{2\pi}\prod_{i=1}^{n}\cos\left(\frac{D_i\tau\pi}{2}\sin 2\beta_i \sin\alpha_i\right)\sin\beta\, d\alpha\, d\beta\, d\gamma \quad , \tag{S1}$$

where D_i corresponds to the dipolar coupling constant between the observed nucleus and the recoupled spin 'i', α_i and β_i are the polar angles orienting this internuclear vector in the magnetic field, τ is the recoupling time, and α, β, and γ are the Euler angles describing the orientation of the crystallite, and rotor phase, in the magnetic field; these three angles are powder averaged. Since the powder averaging must be performed on only a single internuclear vector, the orientations of the other dipolar coupling vectors need to be related to those of the powder averaged one. The orientation of these spin pairs is then related to the powder-averaged pair using two new polar angles (θ_i and φ_i). In this case, the $\sin 2\beta_i \sin\alpha_i$ term from eq 1 is replaced with

$$\sin 2\beta_i \sin\alpha_i = 2\left[\begin{array}{l}\left(\left[\sin\beta\cos\alpha\right]x + \left[\sin\beta\sin\alpha\right]y + \left[\cos\beta\right]z\right) \\ \times\left(\begin{array}{l}\left[-\cos\gamma\sin\alpha - \cos\beta\cos\alpha\sin\gamma\right]x \\ +\left[\cos\gamma\cos\alpha - \cos\beta\sin\alpha\sin\gamma\right]y + \left[\sin\gamma\sin\beta\right]z\end{array}\right)\end{array}\right], \tag{S2}$$

where

$$x = \sin\theta_i\cos\varphi_i \tag{S3}$$

$$y = \sin\theta_i\sin\varphi_i \tag{S4}$$

$$z = \cos\theta_i \tag{S5}$$

---

[6] D. Lee, G. Monin, N. T. Duong, I. Z. Lopez, M. Bardet, V. Mareau, L. Gonon and G. De Paëpe, *J. Am. Chem. Soc.* 2014, **136**, 13781-13788.

[7] T. Kobayashi, D. Singappuli-Arachchige, Z. Wang, I. I. Slowing and M. Pruski, *Phys. Chem. Chem. Phys.* 2017, **19**, 1781-1789.

[8] T. Kobayashi, K. Mao, P. Paluch, A. Nowak-Król, J. Sniechowska, Y. Nishiyama, D. T. Gryko, M. J. Potrzebowski and M. Pruski, *Angew. Chem. Int Ed.* 2013, **52**, 14108-14111.

[9] M. P. Hanrahan, A. Venkatesh, S. L. Carnahan, J. L. Calahan, J. W. Lubach, E. J. Munson and A. J. Rossini, *Phys. Chem. Chem. Phys.* 2017, **19**, 28153-28162.

We have adapted this equation for RESPDOR experiments, which are far more robust in the case of quadrupolar nuclei. For RESPDOR experiments performed on spin-5/2 nuclei, such as ^{27}Al, eq 1 becomes

$$\frac{\Delta S}{S_0} = 1 - \frac{f}{4\pi}\int_0^{2\pi}\int_0^{\pi}\int_0^{2\pi}\prod_{i=1}^{n}\left[\begin{array}{l}\frac{1}{6}+\frac{5}{18}\cos\left(\frac{D_i\tau\pi}{2}\sin 2\beta_i \sin\alpha_i\right)\\ +\frac{2}{9}\cos\left(D_i\tau\pi\sin 2\beta_i \sin\alpha_i\right)\\ +\frac{1}{6}\cos\left(\frac{3D_i\tau\pi}{2}\sin 2\beta_i \sin\alpha_i\right)\\ +\frac{1}{9}\cos\left(2D_i\tau\pi\sin 2\beta_i \sin\alpha_i\right)\\ +\frac{1}{18}\cos\left(\frac{5D_i\tau\pi}{2}\sin 2\beta_i \sin\alpha_i\right)\end{array}\right]\sin\beta\, d\alpha\, d\beta\, d\gamma, \qquad \text{(S6)}$$

where we consider the 6 zero-quantum transitions, 10 single-quantum transitions, 8 double-quantum transition, 6 triple-quantum transitions, 4 quadruple-quantum transitions and 2 quintuple-quantum transitions as equally probable. An additional factor (*f*) is included to both compensate for incomplete saturation and, in our case, the existence of isolated spins that do not dephase. Using eq S6, the RESPDOR dephasing curve for a spin system of arbitrary size can be calculated within a few seconds, in contrast to other costly spin dynamics simulations.

Supplementary Figures

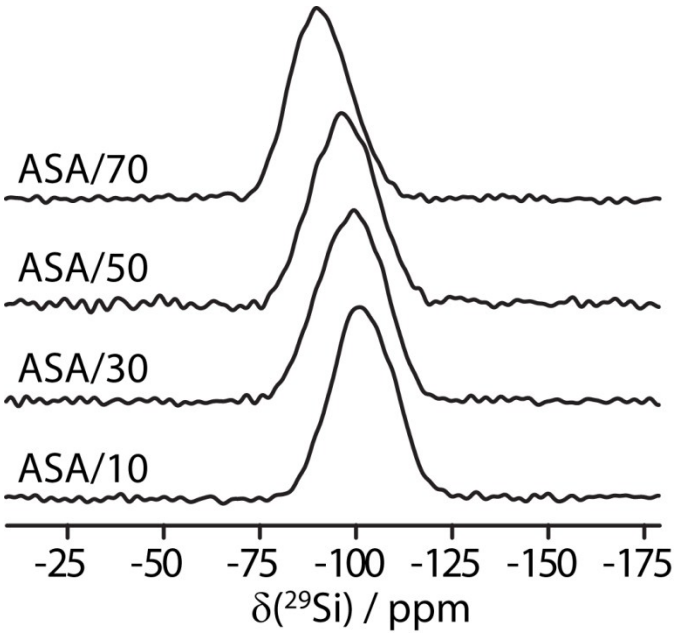

Figure S1. The DNP-enhanced ^{29}Si CPMAS spectra of the ASA samples are shown as a function of the aluminum concentration, as indicated on the Figure.

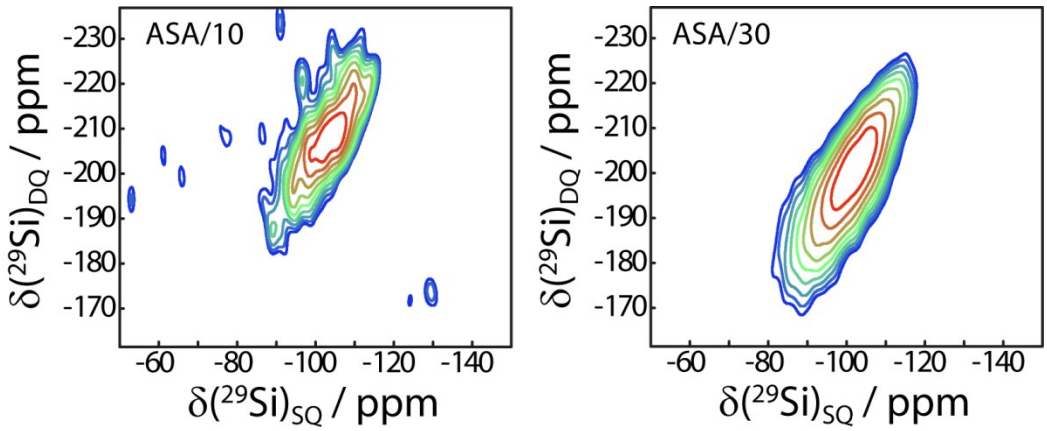

Figure S2. DNP-enhanced ^{29}Si DQ/SQ spectra of ASA samples with different concentrations of aluminum, as indicated on the Figure.

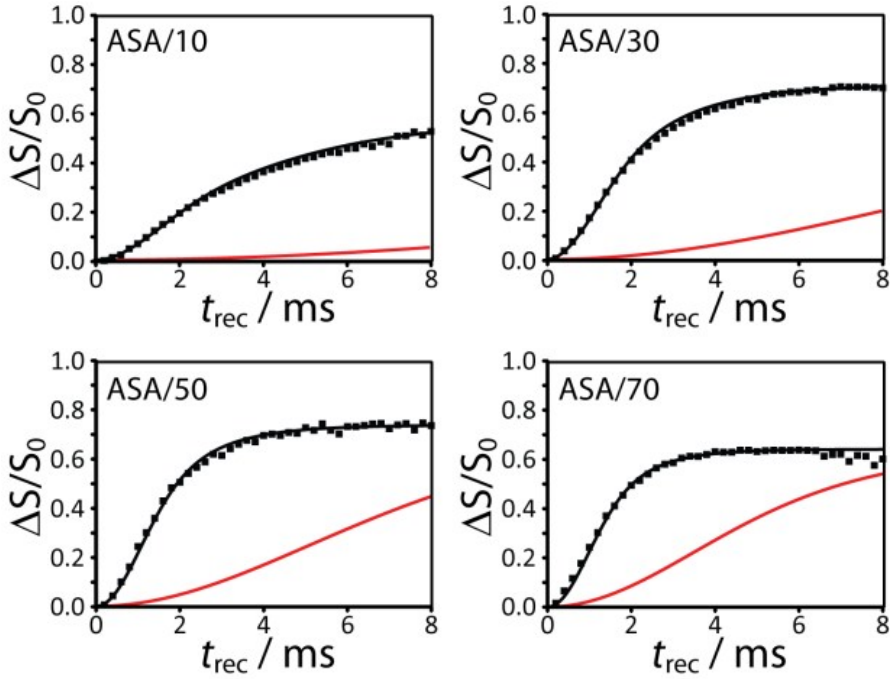

Figure S3. DNP-enhanced ^{29}Si{^{27}Al} RESPDOR curves for the ASA samples discussed in the text. These are fit using a homogeneous model that favors Al avoidance (black). Fits calculated using a purely homogeneous model, with the same parameters, are shown in red.

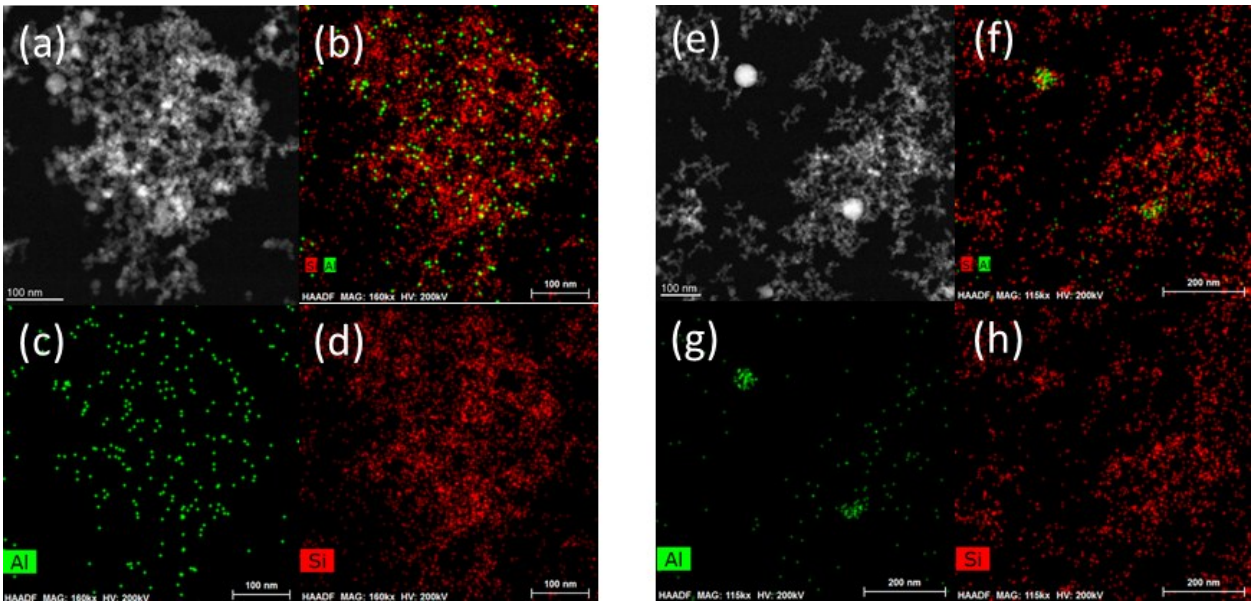

Figure S4. STEM (a, e) and EDX (b-d, f-h) images of two regions of the ASA/10 sample. The Al and Si EDX maps are given in (c, g) and (d, h) and are overlaid in (b, f). The region on the right (e-h) demonstrates the formation of silica-alumina particles with a 50:50 Al:Si ratio.

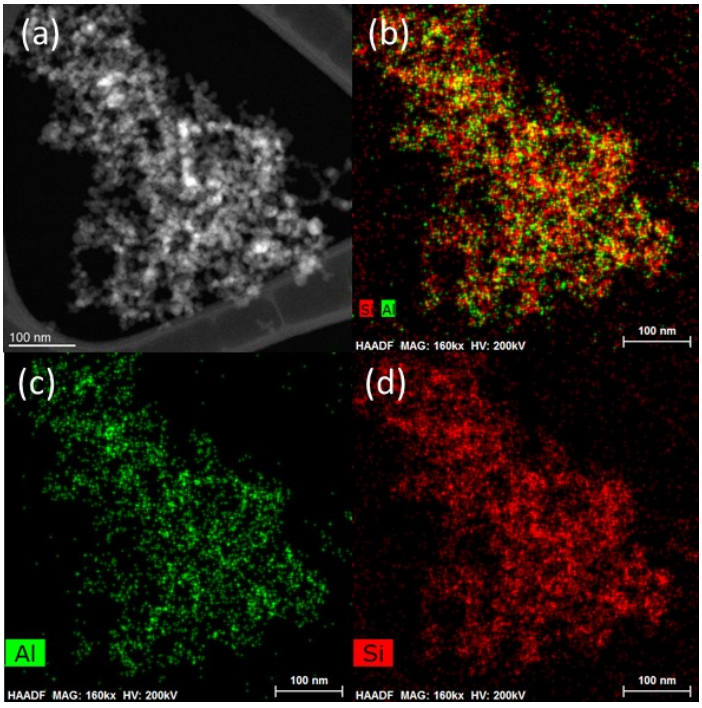

Figure S5. STEM (a) and EDX (b-d) images of the ASA/30 sample. The Al and Si EDX maps are given in (c) and (d) and are overlaid in (b).

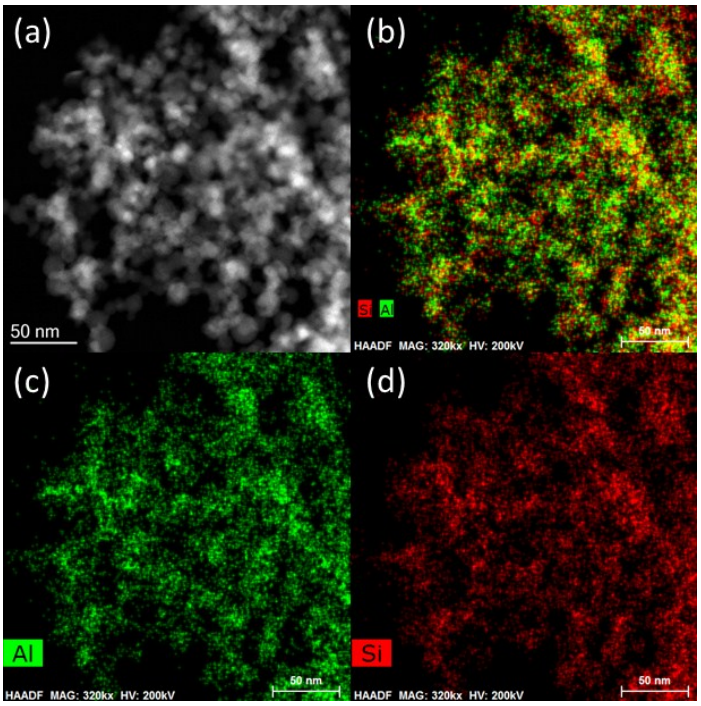

Figure S6. STEM (a) and EDX (b-d) images of the ASA/50 sample. The Al and Si EDX maps are given in (c) and (d) and are overlaid in (b).

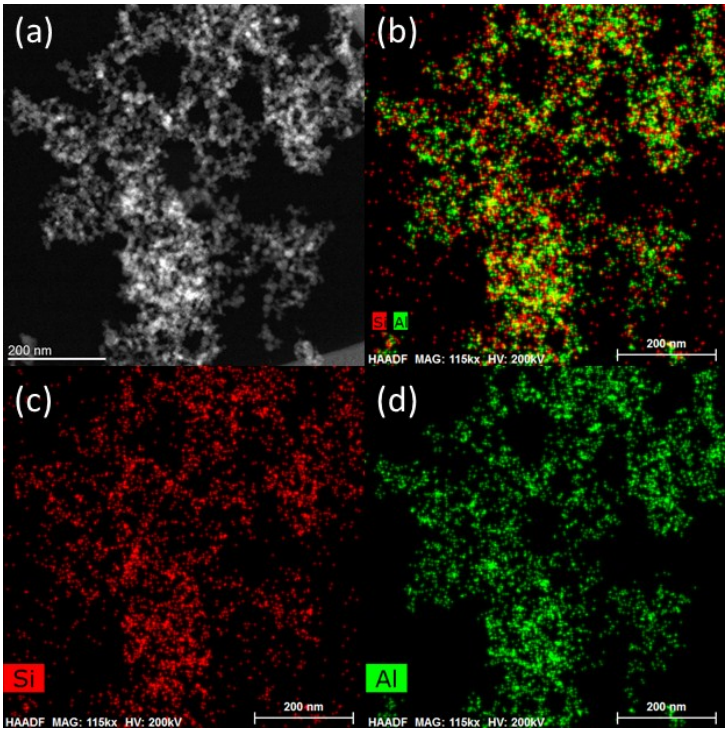

Figure S7. STEM (a) and EDX (b-d) images of the ASA/70 sample. The Al and Si EDX maps are given in (c) and (d) and are overlaid in (b).

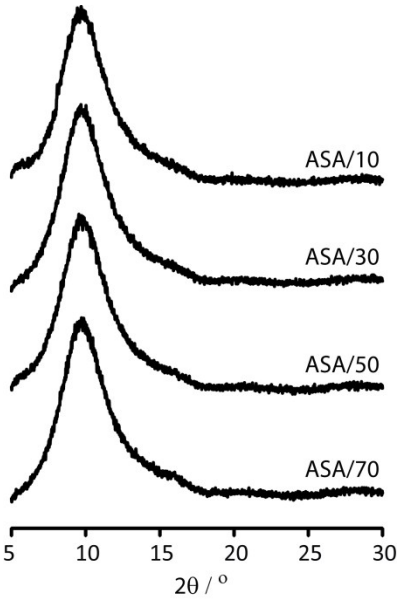

Figure S8. X-ray diffraction patterns for the ASA samples discussed in the main text, as labeled on the Figure.

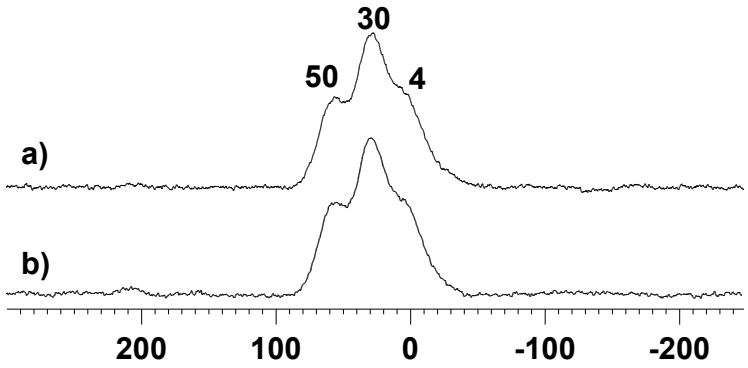

Figure S9. ^{27}Al direct excitation MAS spectra of ASA/50 recorded at 9.4 T with ν_R = 8 kHz: (a) sample dehydrated at 723 K for 12 h under vacuum, and (b) recorded after subsequent heating in O_2 gas atmosphere at 853 K for 12 h on a vacuum line.

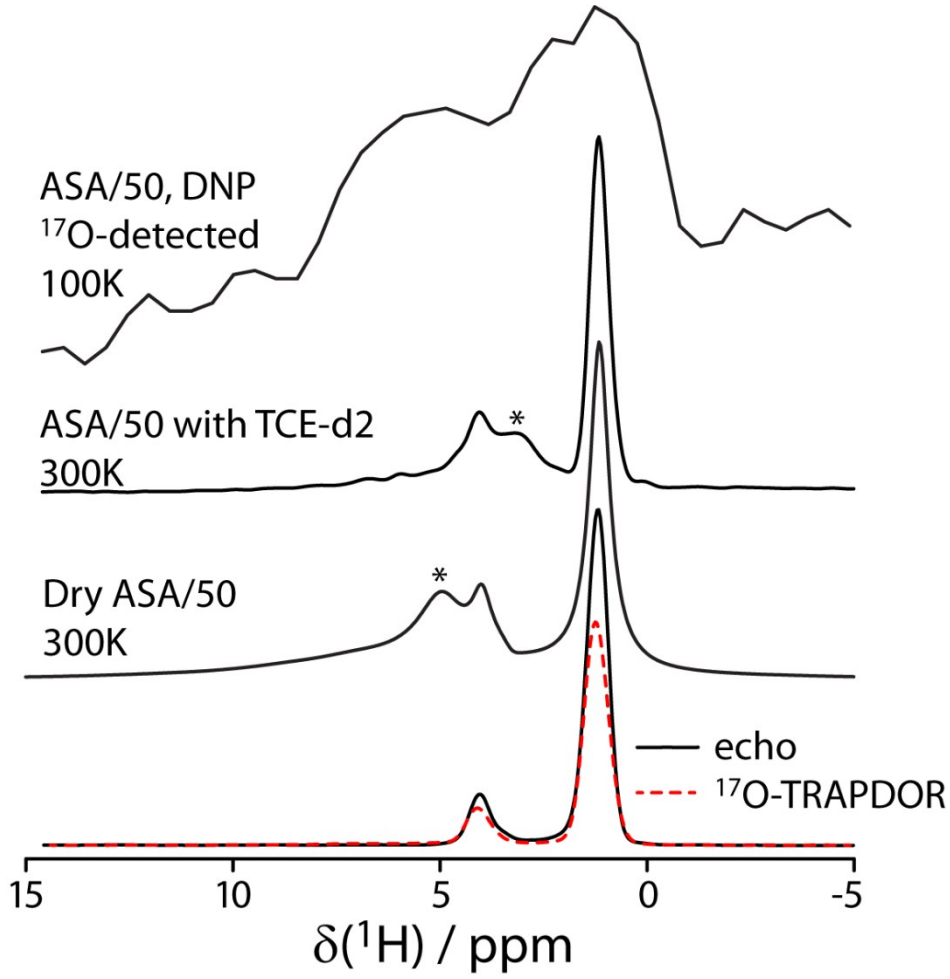

Figure S10. Room temperarure ^{1}H Hahn echo spectra (t_{echo} = 2 ms) of ^{17}O-enriched, ASA/50 material (impregnated in deuterated TCE-d2 and dry) are compared with the ^{1}H projection of the 3D ^{17}O{^{1}H} PDLF-HETCOR spectrum from Figure 4b (shown on top). The corresponding ^{17}O-TRAPDOR-dephased spectrum of the dry material is also shown at the bottom (dashed, red). An asterisk denotes the position of the resonance from physisorbed water, shifts in the presence of TCE due to its weakened hydrogen bonding. This resonance also has a short T_2 and does not appear in the TRAPDOR spectra which used a longer echo delay of 2 ms.

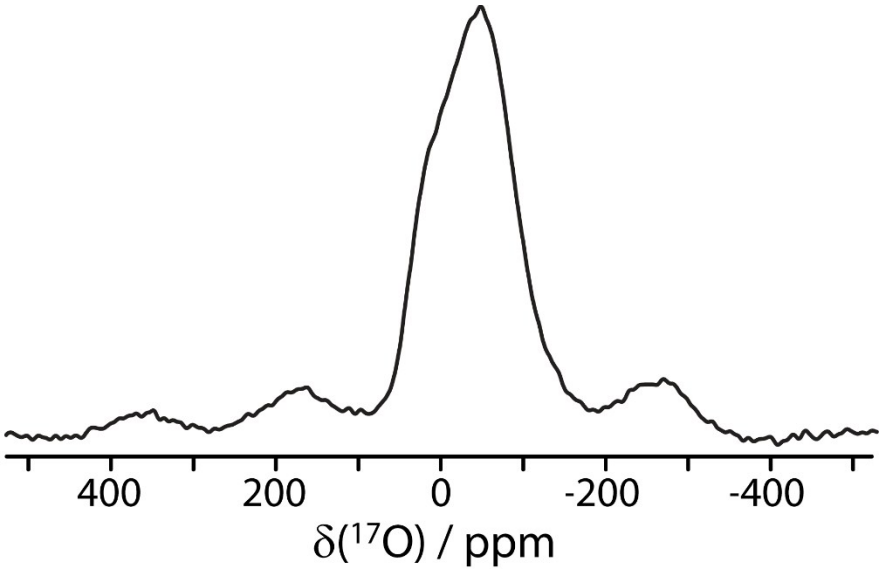

Figure S11. DNP-enhanced $^{17}O\{^{1}H\}$ PRESTO NMR spectrum of the ^{17}O-enriched, ASA/50 material.

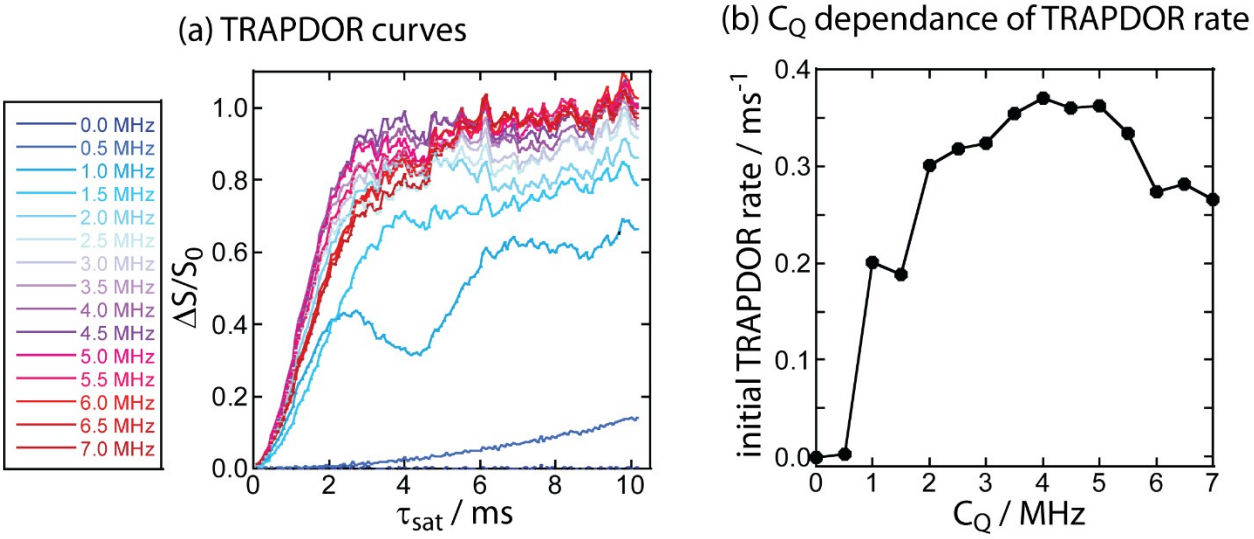

Figure S12. Simulated $^{17}O\{^{27}Al\}$ TRAPDOR curves are plotted for different ^{27}Al C_Q values, as shown in the legend (a). The initial rates (from 0 to 2 ms) are plotted in (b) as a function of the ^{27}Al C_Q value. The rates are relatively constant for the C_Q values above 2 MHz. The dipolar coupling constant was set to 300 Hz for all simulations.